EFT interpretation of $b \to d\,\ell\ell$ decays

Héctor Gisbert

U. Padova & INFN

Based on 2109.01675 & 2209.04457.

In collaboration with R. Bause, M. Golz and G. Hiller.

LHC EFT WG 6 meeting, CERN, November 21, 2022

Rare decays probing BSM physics

- **FCNCs are loop and CKM suppressed in the SM.**

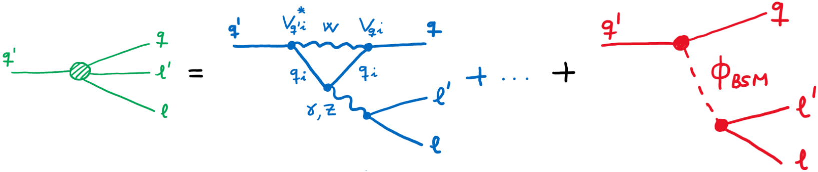

- **BSM contributions could be of same size as the SM.**

Bonus if ℓ are attached (rare decays):

- **SM lepton couplings are flavour universal, LU can be tested.**
- **If $\ell \neq \ell'$ (zero in the SM), LFC can be tested as well.**

Excellent place to search for BSM physics!

EFT approach to rare B decays

1. **Symmetries to build all O_i up to desired dimension ($D=6$):**

$$\mathcal{H}_{\rm eff} \supset \frac{4\,G_F}{\sqrt{2}}\,V_{tq}^* V_{tb}\,\frac{\alpha_e}{4\pi}\sum_i c_i^{(\prime)}\,O_i^{(\prime)}\,, \qquad c_i = C_i^{{\rm SM}(\prime)} + C_i^{(\prime)}\,,$$

$$\begin{aligned} O_7^{(\prime)} &= \frac{e}{16\pi^2}\,m_b\,(\bar{q}_{L\,(R)}\,\sigma_{\mu\nu}\,b_{R\,(L)})\,F^{\mu\nu}\,,\\ O_8^{(\prime)} &= \frac{g_s}{16\pi^2}\,m_b\,(\bar{q}_{L\,(R)}\,\sigma_{\mu\nu}\,T^a b_{R\,(L)})\,G_a^{\mu\nu}\,,\\ O_{9\,(10)}^{(\prime)} &= (\bar{q}_{L\,(R)}\gamma_\mu b_{L\,(R)})(\bar{\ell}\,\gamma^\mu(\gamma_5)\,\ell)\,,\ldots \end{aligned}$$

2. **Compute $C_i(\mu_{\rm EW})$ and RGEs to go down $\mu_{\rm low}\approx m_b$.**

$$C_7^{\rm SM}(m_b)\approx -0.3\,,\; C_8^{\rm SM}(m_b)\approx -0.15\,,\; C_9^{\rm SM}(m_b)\approx 4.1\,,\; C_{10}^{\rm SM}(m_b)\approx -4.2\,.$$

3. **$\langle O_i(\mu_{\rm low})\rangle$ from non-perturbative techniques (Lattice, LCSR, ...)**

4. **Include resonances (or better avoid them).**

An intriguing pattern in $b \to s\,\ell\ell$ transitions

- **Over the past decade a set of tensions with SM predictions has emerged in $b \to s\,\ell\ell$ transitions:**

  1. **Branching ratios:** are below the SM values.
  2. **Angular obserbables:** $4\,\sigma$ deviation from the SM in global fits.
  3. **LU ratios:** $e - \mu$ universality violation has been evidenced by LHCb in R_K, strengthening the trend in measurements of R_K-like ratios.

- **Interestingly, 1 - 3 can be explained consistently together by NP contribution in a single operator:**

$$C_9^{(bs)} \cdot O_9^{bs} \approx -1 \cdot (\bar{s}_L \gamma_\mu b_L)(\bar{\ell}\,\gamma^\mu\,\ell)$$

- **While this strongly points to NP, further scrutiny is required before firm conclusions can be drawn.**

Shedding some light on the flavor anomalies

- **Differences between $b \to d\,\ell\ell$ & $b \to s\,\ell\ell$ in the SM:**

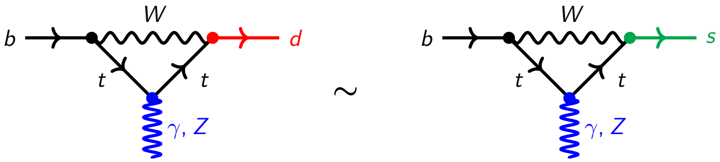

(1) CKM matrix elements: V_{td} vs V_{ts}, **(2)** Light quark masses: m_d vs m_s

$$C_i^{(b\to d)} \approx C_i^{(b\to s)}\,,\ \text{(CKMs factorized in } \mathcal{H}_{\text{eff}})$$

$$C_i'^{(b\to d)} \approx \left(\frac{m_d}{m_s}\right) C_i'^{(b\to s)}\,,\ (O_i' \text{ chiral suppression})$$

- **A violation would signal additional BSM sources of quark flavor violation (beyond (1) and (2)); an agreement would indicate similar effects as the current flavor anomalies (maybe NP?).**

Global fit of $b \to d\,\ell\ell$ transitions

What observables do we use?

- **Branching ratios of rare $b \to d\,\mu^+\mu^-, \gamma$ decays:**
  1. $B^+ \to \pi^+\,\mu^+\mu^-$ (3 binned), 1509.00414.
  2. $B_s^0 \to \bar{K}^{*0}\mu^+\mu^-$ (full integrated), 1804.07167.
  3. $B^0 \to \mu^+\mu^-$, 2108.09283.
  4. $\bar{B} \to X_d\gamma$, 1005.4087,1503.01789.
- **In total we use 6 observables, compared with $b \to s\,\ell\ell$ transitions:**

$$\frac{\#\text{ obs. exp. } (b \to d\,\ell\ell)}{\#\text{ obs. exp. } (b \to s\,\ell\ell)} \sim \frac{1}{50} \text{ (ideally 1)}$$

$B^+ \to \pi^+ \mu^+ \mu^-$

2209.04457

k	$[q^2_{\min}, q^2_{\max}]$ [GeV^2]	$\mathcal{B}_k^{(B\pi)}$ SM [10^{-9} GeV^{-2}]	$\mathcal{B}_k^{(B\pi)}$ experiment [10^{-9} GeV^{-2}]
1	$[2, 4]$	$0.80 \pm 0.12 \pm 0.05 \pm 0.04$	$0.62^{+0.39}_{-0.33} \pm 0.02$
		FFs CKMs scale	stat. syst.
2	$[4, 6]$	$0.81 \pm 0.12 \pm 0.05 \pm 0.05$	$0.85^{+0.32}_{-0.27} \pm 0.02$
3	$[6, 8]$	$0.82 \pm 0.11 \pm 0.05 \pm 0.07$	$0.66^{+0.30}_{-0.25} \pm 0.02$
4	$[11, 12.5]$	$0.82 \pm 0.09 \pm 0.05 \pm 0.09$	$0.88^{+0.34}_{-0.29} \pm 0.03$
5	$[15, 17]$	$0.73 \pm 0.06 \pm 0.04 \pm 0.06$	$0.63^{+0.24}_{-0.19} \pm 0.02$
6	$[17, 19]$	$0.67 \pm 0.05 \pm 0.04 \pm 0.05$	$0.41^{+0.21}_{-0.17} \pm 0.01$
7	$[19, 22]$	$0.57 \pm 0.03 \pm 0.03 \pm 0.04$	$0.38^{+0.18}_{-0.15} \pm 0.01$
8	$[22, 25]$	$0.35 \pm 0.02 \pm 0.02 \pm 0.02$	$0.14^{+0.13}_{-0.09} \pm 0.01$
9	$[15, 22]$	$0.64 \pm 0.04 \pm 0.04 \pm 0.05$	$0.47^{+0.12}_{-0.10} \pm 0.01$
10	$[4m_\mu^2, (m_{B^+} - m_{\pi^+})^2]$	$17.9 \pm 1.9 \pm 1.1 \pm 1.5^\dagger$ GeV^2	$18.3 \pm 2.4 \pm 0.5$ GeV^2

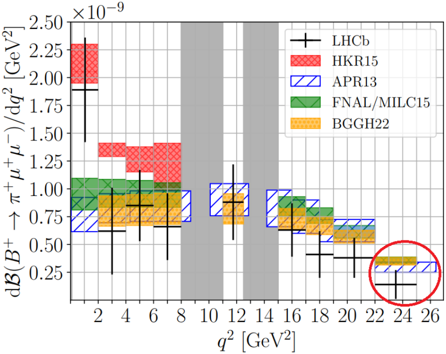

- Very good agreement (below 1 σ) except for $[22, 25]$ GeV^2 with 1.6 σ.
- Low-q^2 bin [0.1, 2] GeV^2, suffers from ρ, ω and ϕ resonances.
- $q^2 \approx 9.5$ GeV^2 & $q^2 \approx 13.5$ GeV^2 suffer from J/ψ and ψ resonances.
- Only include the theoretically clean bins: [2, 4], [4, 6], [15, 22] GeV^2.

$$\mathcal{B}(B_s^0 \to \bar{K}^{*0}\mu^+\mu^-)_{\rm SM} = (46.0 \pm 6.0)\cdot 10^{-9}$$

FFs CKM scale resonances

$$= (46.0 \pm 2.1 \pm 2.8 \pm 3.3 \pm 3.6)\cdot 10^{-9}$$

2209.04457

1.4 σ >

$$\mathcal{B}(B_s^0 \to \bar{K}^{*0}\mu^+\mu^-)_{\rm exp} = (29 \pm 11)\cdot 10^{-9}$$

1804.07167

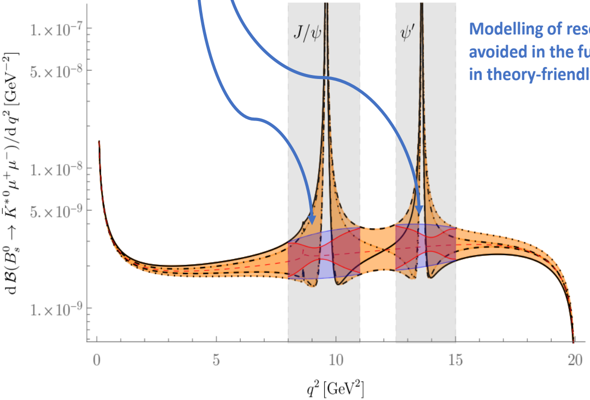

Modelling of resonances can be avoided in the future with data in theory-friendly bins!

$B^0 \to \mu^+\mu^-$ and scalar operators

- In the SM, only the operator O_{10} contributes which yields

$$\mathcal{B}(B^0 \to \mu^+\mu^-)_{\text{SM}} = (1.14 \pm 0.12) \cdot 10^{-10} \,,$$
$$\mathcal{B}(B^0 \to \mu^+\mu^-)_{\text{exp}} = (1.20 \pm 0.84) \cdot 10^{-10} \,,$$

  in agreement with the experimental value 2108.09283.
- $\mathcal{B}(B^0 \to \mu^+\mu^-)$ is sensitive to $O_{10}^{(\prime)}$, $O_S^{(\prime)}$, and $O_P^{(\prime)}$ operators.

$$\frac{\mathcal{B}(B^0 \to \mu^+\mu^-)}{\mathcal{B}(B^0 \to \mu^+\mu^-)_{\text{SM}}} = |\mathcal{P}|^2 + |\mathcal{S}|^2$$

$$\mathcal{P} = \frac{C_{10}^{\text{SM}} + C_{10-}}{C_{10}^{\text{SM}}} + \frac{m_B^2}{2\,m_\mu}\left(\frac{1}{m_b + m_d}\right)\left(\frac{C_{P-}}{C_{10}^{\text{SM}}}\right)$$
$$\mathcal{S} = \frac{m_B^2}{2\,m_\mu}\sqrt{1 - \frac{4m_\mu^2}{m_B^2}}\left(\frac{1}{m_b + m_d}\right)\left(\frac{C_{S-}}{C_{10}^{\text{SM}}}\right) .$$

- Using the current experimental information

$$-1.4 \lesssim C_{10-} \lesssim 1.9 \quad \text{or} \quad 6.5 \lesssim C_{10-} \lesssim 9.8$$
$$-0.05 \lesssim C_{P-} \lesssim 0.06 \quad \text{or} \quad 0.2 \lesssim C_{P-} \lesssim 0.3$$
$$|C_{S-}| \lesssim 0.1\,,$$

- $O_S^{(\prime)}$, and $O_P^{(\prime)}$ are more constrained than $O_{10}^{(\prime)}$ (due to m_B/m_μ) not considered in the global fits.

$\bar{B} \to X_d\gamma$

- The SM prediction for the CP-averaged $\bar{B} \to X_d\gamma$ branching ratio

$$\mathcal{B}(\bar{B} \to X_d\gamma)_{\rm SM} = (17.7 \pm 1.7) \cdot 10^{-6} \ ,$$
$$\mathcal{B}(\bar{B} \to X_d\gamma)_{\rm exp} = (14.1 \pm 5.7) \cdot 10^{-6} \ ,$$

in very good agreement.

- $\mathcal{B}(\bar{B} \to X_d\gamma)$ is sensitive to $O_7^{(\prime)}$ and $O_8^{(\prime)}$ operators.

$$\mathcal{B}(\bar{B} \to X_d\gamma) = \sum_{i=1}^{9} a_i^{(\bar{B}X_d)} w_i^{(\bar{B}X_d)}$$

$$w_i^{(\bar{B}X_d)} = \{1,\, C_7,\, C_8,\, C_7^2,\, C_8^2,\, (C_7')^2,\, (C_8')^2,\, C_7 \cdot C_8,\, C_7' \cdot C_8'\}$$

In units of 10^{-5}

$a_1^{(\bar{B}X_d)}$	$a_2^{(\bar{B}X_d)}$	$a_3^{(\bar{B}X_d)}$
1.77	−3.72	−0.91
$a_4^{(\bar{B}X_d)} = a_6^{(\bar{B}X_d)}$	$a_5^{(\bar{B}X_d)} = a_7^{(\bar{B}X_d)}$	$a_8^{(\bar{B}X_d)} = a_9^{(\bar{B}X_d)}$
2.60	0.25	1.22

Fit approach

We work within a frequentist framework based on the approximation of Gaussian likelihood

$$\mathcal{L}(\theta) = \mathrm{e}^{-\chi^2(\theta)/2}$$

Wilson coefficients

$$\chi^2(\theta) = -2\ln\mathcal{L}(\theta) = \sum_{i,j}^{n_{\rm obs}} \Delta_i(\theta)\, V_{ij}^{-1}(\theta)\, \Delta_j(\theta)\,,$$

Central values: $\Delta_i(\theta) = \Delta_i^{(\rm th)}(\theta) - \Delta_i^{(\rm exp)}\,,$

Covariance matrix: $V_{ij}(\theta) = V_{ij}^{(\rm th)}(\theta) + V_{ij}^{(\rm exp)}\,.$

Usually WCs=0, here the experimental is less stringent so it is important to include these effects.

6 observables

$$\vec{\Delta} = \{\mathcal{B}_1^{(B\pi)}, \mathcal{B}_2^{(B\pi)}, \mathcal{B}_9^{(B\pi)}, \mathcal{B}(B_s^0 \to \bar{K}^{*0}\mu^+\mu^-), \mathcal{B}(B^0 \to \mu^+\mu^-), \mathcal{B}(\bar{B} \to X_d\gamma)\}\,.$$

Minimization of chi-square: Maximum likelihood method $\partial\chi^2/\partial\theta_i|_{\hat{\theta}} = 0 \longrightarrow \hat{\theta}$ Best-fit points

Confidence regions: $\Delta\chi^2(\theta) \leq \eta\,(l, n_{\rm par})$ where $\Delta\chi^2(\theta) = \chi^2(\theta) - \chi^2_{\rm min}$

Value where the chi-square cumulative distribution function reaches the probability associated with l sigmas

$\eta\,(l,1) = l^2,\ \eta\,(l,2) = (2.30, 6.18, \ldots),$ etc.

In practice:
* MIGRAD from the Python package iminuit to conduct the numerical minimization.
* Confidence intervals are computed using MINOS algorithm from iminuit.

One-dimensional fits

scenario	fit parameter	best fit	1σ	2σ	$\chi^2_{H_i,\,\min}$	Pull_{H_i}	p-value (%)
H_1	C_7	0.01	[-0.11, 0.15]	[-0.23, 0.31]	3.87	0.10	56
H_2	C_8	0.31	[-0.31, 1.42]	[-0.82, 4.05]	3.66	0.47	59
H_3	C_9	-1.37	[-2.97, -0.47]	[-7.65, 0.26]	1.23	1.63	94
H_4	C_{10}	0.96	[0.31, 1.74]	[-0.27, 2.88]	1.55	1.53	90
H_5	C_7'	-0.03	[-0.22, 0.19]	[-0.39, 0.39]	3.86	0.12	56
H_6	C_8'	-0.03	[-1.15, 1.11]	[-1.89, 1.87]	3.88	0.02	56
H_7	C_9'	-0.21	[-0.91, 0.47]	[-1.63, 1.15]	3.78	0.32	58
H_8	C_{10}'	0.18	[-0.40, 0.75]	[-0.99, 1.32]	3.78	0.31	58
H_9	$C_9 = +C_{10}$	0.24	[-0.52, 1.04]	[-1.18, 1.79]	3.79	0.30	58
H_{10}	$C_9 = -C_{10}$	-0.54	[-0.90, -0.20]	[-1.29, 0.13]	1.32	1.60	93
H_{11}	$C_9' = +C_{10}'$	0.05	[-0.72, 0.79]	[-1.43, 1.45]	3.88	0.06	56
H_{12}	$C_9' = -C_{10}'$	-0.12	[-0.45, 0.23]	[-0.78, 0.58]	3.76	0.34	58
H_{13}	$C_9 = -C_9'$	-1.74	[-3.26, -0.27]	[-4.04, 0.44]	2.08	1.34	83
H_{14}	$C_9 = +C_9'$	-0.55	[-1.29, -0.07]	[-4.13, 0.34]	2.53	1.16	77
H_{15}	$C_9 = -C_{10} = -C_9' = -C_{10}'$	-0.58	[-1.06, -0.20]	[-4.04, 0.12]	1.28	1.61	93
H_{16}	$C_9 = -C_{10} = +C_9' = -C_{10}'$	-0.24	[-0.46, -0.04]	[-0.70, 0.16]	2.47	1.19	78

What do we learn from the one-dimensional fits?

- The most favored scenario is H_3 NP in C_9 (pull=1.63, p-value=94%), followed by H_4 with NP in C_{10} (pull=1.53, p-value=90%).
- Scenarios relating 2 WCs (H_9,...,H_{14}):
  1. H_{10} with LH quarks and LH leptons, $C_9 = -C_{10}$, is preferred by data (pull=1.60, p-value=93%). For comparison, we explore benchmark H_9, LH quarks and RH leptons $C_9 = C_{10}$, results are close to the SM.
  2. We work correlations in $C'_{9,10}$ and find p-values closer to the SM one.
  3. We consider $C_9 = \pm C'_9$, where we find similar results (pull≈1.3, p-value≈80%).

⋆ **Consistency with the SM, but data shows a clear preference to include NP via C_9, similar as in global fits to $b \to s\,\mu^+\mu^-$ data.**

⋆ **Future data is very welcome to confirm or refute this pattern!**

Let's further entertain with two-dimensional fits!

scen.	fit parameters	best fit	1σ	2σ	$\chi^2_{H_i,\,\mathrm{min}}$	Pull_{H_i}	p-v. (%)
H_{17}	(C_7, C_8)	(-0.22, 1.47)	([-0.46, 0.08], [-0.2, 3.73])	([-0.64, 0.36], [-1.36, 4.6])	3.14	0.40	53
H_{18}	(C_7, C_9)	(0.11, -1.55)	([-0.05, 0.34], [-3.05, -0.61])	([-0.18, 1.46], [-10.07, 0.18])	0.77	1.25	94
H_{19}	(C_7, C_{10})	(0.09, 1.1)	([-0.07, 0.28], [0.39, 2.04])	([-0.2, 0.55], [-0.23, 8.64])	1.25	1.10	86
H_{20}	(C_7, C'_7)	(0.01, -0.03)	([-0.11, 0.16], [-0.23, 0.19])	([-0.23, 0.31], [-0.41, 0.4])	3.85	0.02	42
H_{21}	(C_7, C'_9)	(0.02, -0.23)	([-0.11, 0.16], [-0.92, 0.46])	([-0.23, 0.32], [-1.64, 1.16])	3.76	0.07	43
H_{22}	(C_7, C'_{10})	(0.02, 0.19)	([-0.11, 0.16], [-0.39, 0.77])	([-0.23, 0.32], [-0.99, 1.35])	3.76	0.07	43
H_{23}	(C_9, C_{10})	(-1.28, 8.34)	([-7.54, 0.71], [6.39, 9.31])	([-9.12, 1.85], [-1.38, 9.79])	1.12	1.14	89
H_{24}	(C'_7, C_9)	(0.08, -1.43)	([-0.2, 0.35], [-2.97, -0.5])	([-0.53, 0.55], [-7.64, 0.26])	1.17	1.13	88
H_{25}	(C_9, C'_9)	(-2.22, 1.18)	([-6.55, -0.63], [-2.99, 2.89])	([-7.58, 0.23], [-3.92, 3.81])	0.87	1.22	92
H_{26}	(C_9, C'_{10})	(-1.83, -0.38)	([-6.58, -0.6], [-1.2, 0.32])	([-7.6, 0.25], [-1.8, 0.99])	0.95	1.20	91
H_{27}	(C'_7, C_{10})	(0.06, 1.01)	([-0.19, 0.33], [0.33, 1.92])	([-0.38, 0.55], [-0.27, 2.53])	1.50	1.03	82
H_{28}	(C'_9, C_{10})	(0.26, 1.09)	([-0.52, 1.03], [0.34, 2.12])	([-1.32, 1.81], [-0.28, 8.7])	1.44	1.05	83
H_{29}	(C_{10}, C'_{10})	(0.97, -0.04)	([0.3, 1.87], [-1.0, 0.72])	([-0.29, 2.45], [-4.52, 4.48])	1.54	1.01	81
H_{30}	(C'_7, C'_9)	(0.03, -0.28)	([-0.23, 0.28], [-1.15, 0.62])	([-0.45, 0.49], [-2.01, 1.51])	3.77	0.07	43
H_{31}	(C'_7, C'_{10})	(0.0, 0.18)	([-0.22, 0.23], [-0.45, 0.8])	([-0.4, 0.42], [-1.09, 1.41])	3.78	0.06	43
H_{32}	(C'_9, C'_{10})	(-0.13, 0.11)	([-1.11, 0.77], [-0.68, 0.89])	([-2.06, 1.57], [-1.41, 1.64])	3.76	0.07	43
H_{33}	$(C_9 = -C'_9,\, C_{10} = +C'_{10})$	(-1.73, 0.44)	([-3.34, -0.19], [0.04, 0.95])	([-4.1, 0.51], [-0.34, 4.52])	0.88	1.22	92
H_{34}	$(C_9 = -C'_9,\, C_{10} = -C'_{10})$	(-1.73, 0.05)	([-3.69, 0.18], [-0.4, 0.94])	([-4.59, 1.04], [-0.79, 5.0])	2.07	0.83	72
H_{35}	$(C_9 = +C'_9,\, C_{10} = +C'_{10})$	(0.6, 2.18)	([0.26, 0.89], [-0.58, 4.77])	([-4.95, 1.19], [-0.92, 5.1])	2.27	0.76	68
H_{36}	$(C_9 = -C_{10},\, C'_9 = +C'_{10})$	(-0.56, 0.37)	([-2.02, -0.2], [-1.39, 2.79])	([-1.36, 0.13], [-2.98, 4.04])	1.27	1.10	86
H_{37}	$(C_9 = -C_{10},\, C'_9 = -C'_{10})$	(-0.61, 0.16)	([-1.07, -0.22], [-0.26, 0.64])	([-1.82, 0.14], [-0.65, 1.43])	1.19	1.13	88

⋆ **Similar pattern as 1D fits, if C_9 present, p-values are large, $\sim$ 90%!**

⋆ **The most favored scenario is H_{18} (pull=1.25, p-value=94%) fitting simultaneously C_7 and C_9.**

2D contours of dipole coefficients

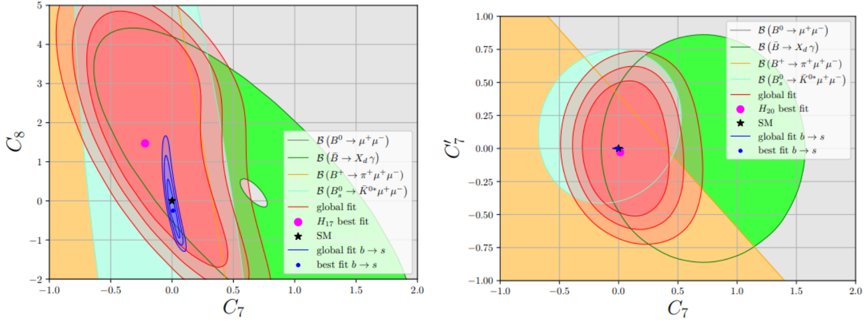

⋆ **Excellent complementarity between different observables!**

⋆ **Improved limits on $C_7^{(\prime)}$ compared to previous works.** 1106.5499

⋆ **Data is consistent with the hypothesis of minimal quark flavor violation.** 2109.01675 & 2209.04457

2D contours of $C^{(\prime)}_{9,10}$

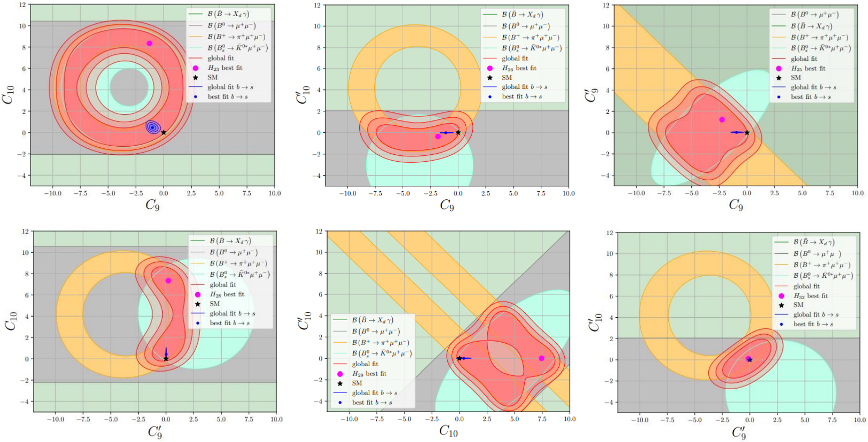

Summary of 2D contours of $C_{9,10}^{(\prime)}$

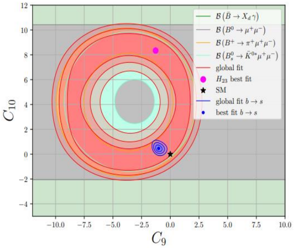

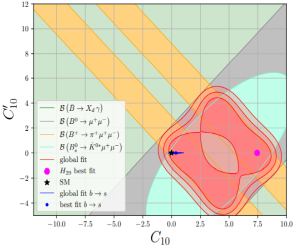

- Complementarity between the observables is not currently as good as for dipole coefficients, leading to weaker limits on C_9 and C_{10} .
- The branching ratios of $B^+ \to \pi^+\mu^+\mu^-$ and $B_s^0 \to \bar{K}^{0*}\mu^+\mu^-$ cooperate to reduce the thickness of the annulus (red area) but do not lift the degeneracy between C_9 and C_{10} .
- The branching ratio of $B^0 \to \mu^+\mu^-$ can help due to its dependence on $C_{10}^{(\prime)}$, however, the present precision is insufficient.
- Note that due to the flat likelihood along the ring (red area) the best-fit point (magenta) is only shown for completeness but has little statistical preference over other points in this flat direction.
- All 2D contours make visible discrete ambiguities, for instance the two yellow bands in C_{10}, C'_{10} .
- To remove all these ambiguities additional complementary observables are necessary.
- Data is consistent with the hypothesis of minimal quark flavor violation.

Conclusions & Outlook

⋆ Model-independent analysis of rare radiative and semileptonic $|\Delta b| = |\Delta d| = 1$ process.

⋆ Data consistent with the SM, but leave sizable room for NP.

⋆ Same pattern of $b \to s\,\mu^+\mu^-$ branching ratios suppressed with respect to the SM, although within larger uncertainties.

⋆ Improving the fit is not just higher statistics, but also of adding observables sensitive to different combinations of WCs.

⋆ Rare $b \to d\,\mu^+\mu^-$ decays can be studied at LHCb, Belle II, and a possible future e^+e^- collider running at the Z.

Thank you!